

DOI: 10.1002/cmdc.200900242

## 2-Acylaminopyridin-4-ylimidazoles as p38 MAP Kinase Inhibitors: Design, Synthesis, and Biological and Metabolic Evaluations

Katharina Ziegler,<sup>[a]</sup> Dominik R. J. Hauser,<sup>[a, b]</sup> Anke Unger,<sup>[b]</sup> Wolfgang Albrecht,<sup>[b]</sup> and Stefan A. Laufer<sup>\*[a]</sup>

Targeting cytokines has become an important focus in the treatment of many inflammatory disorders. p38 MAP kinase (MAPK) is the key enzyme in regulating the biosynthesis and release of pro-inflammatory cytokines such as IL-1 $\beta$  and TNF $\alpha$ . Inhibition of p38 MAPK results in decreased expression of these cytokines. Tri- and tetrasubstituted pyridinylimidazoles are potent inhibitors of p38 MAPK. Substitution on the pyridinyl moiety allows the design of inhibitors that show increased selectivity and activity by targeting the enzyme's hydrophobic region II. The objective of this study was to synthesize novel 1,2,4,5-tetrasubstituted imidazole derivatives and to characterize

them not only for their ability to inhibit p38 MAPK and modulate cytokine release in human whole blood, but also to evaluate their metabolic stability. Biological data and metabolic studies demonstrate that the introduction of a 2-acylamino function at C2 of the pyridine results in highly efficient and metabolically stable inhibitors relative to C2-alkylamino derivatives. A series of novel candidates was investigated for metabolic stability in human liver microsomes and in human whole blood. Additionally, metabolic S-oxidation was investigated, and possible metabolites were synthesized.

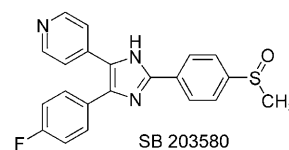
### Introduction

Rheumatoid arthritis (RA) is a ubiquitous, chronic, inflammatory and destructive arthropathy that affects 1% of the world's population.<sup>[1]</sup> The disease is of unknown etiology and cannot be cured. It is a chronic progressive systemic disorder and results in a painful loss of function and deformation of joints. Patients therefore suffer from a severe decrease in the quality of life.<sup>[2]</sup> For this reason it is necessary to start medical treatment at an early stage of the disease. The limited spectrum of therapeutics available for the treatment of the activated state of RA includes corticosteroids and COX-2 inhibitors. In most cases, continuous therapy with disease-modifying anti-rheumatic drugs (DMARDs) is sufficient.<sup>[3]</sup> Patients who do not adequately respond to treatment with a traditional DMARD may respond to cytokine-neutralizing biological agents either in combination therapy with classical DMARDs or in monotherapy. In this context, the turn of the millennium was also a turning point in the treatment of RA. Both the US Food and Drug Administration (FDA) and the European Medicine Evaluation Agency (EMA) approved Etanercept, a soluble tumor necrosis factor  $\alpha$  (TNF $\alpha$ ) type II receptor-IgG fusion protein, and Infliximab, a chimeric (human and mouse) monoclonal antibody against TNF $\alpha$ . These current therapies could dramatically change the treatment and outcome of RA.<sup>[4–17]</sup> At present, many pharmaceutical companies have turned their attention to the development of cytokine-antagonizing drugs that block the release of pro-inflammatory cytokines in an early state of the inflammatory reaction.<sup>[18,19]</sup>

Although the etiology of RA has not been completely elucidated, the mechanisms of inflammation are generally well characterized. Because of the complex network of cellular and

humoral interactions, a broad spectrum of potential therapeutic targets may be addressed. The p38 mitogen-activated protein kinase (MAPK) is well known as the key enzyme in the regulation of the synthesis of pro-inflammatory cytokines such as IL-1 and TNF $\alpha$ ,<sup>[20]</sup> and is therefore an important target for the development of a new class of anti-inflammatory agents.<sup>[21]</sup>

Pyridinylimidazoles such as the prototype SB 203580 are known for potent inhibition of p38 MAPK.<sup>[22]</sup> Inhibitors of this class compete with the original co-substrate ATP for binding in the ATP binding pocket of the kinase.<sup>[3,23]</sup> Unlike the native p38



[a] Dr. K. Ziegler, Dr. D. R. J. Hauser, Prof. Dr. S. A. Laufer  
Institute of Pharmacy, Department of Pharmaceutical and Medicinal  
Chemistry, Eberhard-Karls-University Tübingen, Auf der Morgenstelle 8,  
72076 Tübingen (Germany)  
Fax: (+49) 7071-29-5037  
E-mail: stefan.laufer@uni-tuebingen.de

[b] Dr. D. R. J. Hauser, Dr. A. Unger, Dr. W. Albrecht  
c-a-i-r biosciences GmbH, Paul-Ehrlich-Str. 15, 72076 Tübingen (Germany)

Supporting information for this article is available on the WWW under  
<http://dx.doi.org/10.1002/cmdc.200900242>: Full experimental procedures  
and spectroscopic data for compounds 3–53; HRMS and HPLC data for  
the target compounds.

MAPK co-substrate ATP, pyridinylimidazole inhibitors bind to the active site of both the active (bis-phosphorylated) and inactive forms of the kinase. The essential pharmacophore is the 4-aryl-5-(pyridin-4-yl)imidazole.<sup>[24]</sup> The 4-fluorophenyl moiety of the inhibitor binds in hydrophobic pocket I, where Thr 106 acts as a gatekeeper. In several related kinases, Thr106 is replaced by amino acids with larger side chains (such as Met) which explains the selectivity of inhibitors found in the class of 4-aryl-5-(pyridin-4-yl)imidazoles.<sup>[25]</sup> The pyridin-4-yl moiety is essential for inhibitory potency and generates a crucial hydrogen bond with the backbone amino group of Met 109.<sup>[26]</sup>

Herein we present the synthesis of a series of novel 1,2,4,5-tetrasubstituted imidazole compounds and an evaluation of their inhibitory potency against p38 MAPK and in preventing the release of TNF $\alpha$ . Figure 1 illustrates the active site interactions between p38 MAPK and the general structure of our series of analogues (model modified for p38 from Traxler<sup>[27]</sup>).

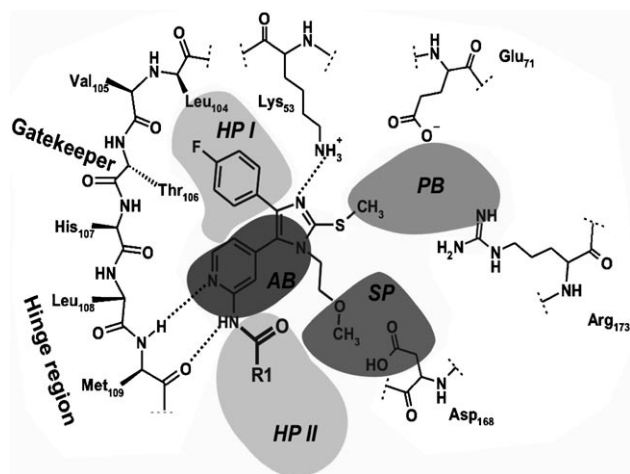


**Figure 1.** Interactions of 2-acylamino-4-ylimidazoles as ATP-competitive compounds with the ATP binding site of p38 MAPK: **AB**, adenine binding region; **SP**, sugar pocket; **PB**, phosphate binding region; **HP I**, hydrophobic region I (also called selectivity pocket) adjacent to Thr 106; and **HP II**, hydrophobic region II, where the cleft opens to the cytosol. (Modified for p38 from Traxler<sup>[27]</sup>.)

## Results and Discussion

### Scaffold design

Previous studies reported 2-alkylamino-4-ylimidazoles as both potent p38 MAPK inhibitors and potent blockers of TNF $\alpha$  release in human whole blood (HWB).<sup>[28,29]</sup> Substitution at the 2-pyridinyl moiety dramatically increases activity and selectivity.<sup>[26,29,30]</sup> Table 1 clarifies the predominance of 1,2,4,5-tetrasubstituted 2-alkylamino-4-ylimidazoles synthesized for comparison with analogous 2-acylamino-4-ylimidazoles in later experiments. Further experiments revealed that compounds of the 2-alkylamino-4-yl series showed instability when incubated with human liver microsomes (HLM) or in HWB. The 2-alkylamino function can be easily cleaved. Hence, the resulting free 2-amino group could be an unspecific target for other metabolic enzymes. Moreover, a loss of activity as well as increasing

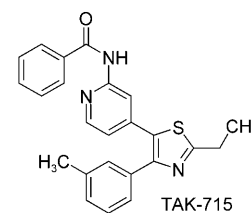
**Table 1.** Inhibition of p38 MAPK and inhibition of TNF $\alpha$  release: biological data for 1,2,4,5-tetrasubstituted 2-alkylamino-4-ylimidazoles in comparison with 2-acylamino-4-ylimidazoles.

Compd	R	IC <sub>50</sub> [ $\mu$ M] <sup>[a]</sup>	
		p38 $\alpha$	TNF $\alpha$
11		0.063 $\pm$ 0.01	36.97 $\pm$ 9.04
17		0.060 $\pm$ 0.01	21.38 $\pm$ 5.69
47		0.026 $\pm$ 0.01	22.35 $\pm$ 3.65
48		0.035 $\pm$ 0.01	17.86 $\pm$ 5.48

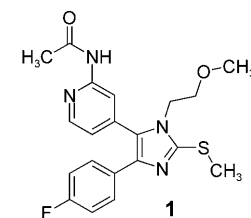
[a] All data listed in Tables 1–7 are the mean values  $\pm$  SEM of three independent experiments.

side effects due to decreased selectivity might be expected. Moieties such as the phenylethylamine group may be easily dealkylated in HLM.<sup>[31,32]</sup>

On the other hand, 2-acylamino-4-ylimidazoles such as TAK-715 show enhanced metabolic stability.<sup>[33]</sup> However, few structure–activity relationships on acyl derivatives within the imidazole series are known, because only the acetyl moiety has been probed so far.<sup>[22,28,34]</sup>



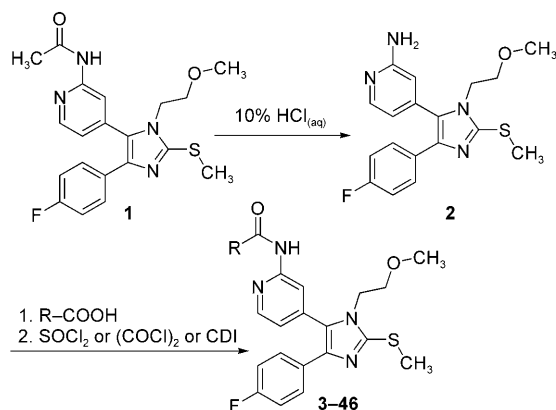
The acetyl group has been incorporated into a series of tetrasubstituted imidazoles in which the imidazole N1 substituent was optimized. This approach resulted in *N*-(4-[5-(4-fluorophenyl)-3-(2-methoxyethyl)-2-methylsulfanyl-3*H*-imidazol-4-yl]pyridin-2-yl)acetamide (**1**) as a potent p38 MAPK inhibitor.<sup>[22]</sup> The current study reports the optimization of the acylamino moiety on pyridine C2 and the evaluation of the metabolic stability of selected compounds.



### Chemistry

The general synthesis of compound **1** has been previously described.<sup>[22,28,34]</sup> Subsequent deacetylation in 10% aqueous hydrochloric acid at reflux gave 4-[5-(4-fluorophenyl)-3-(2-methoxyethyl)-2-methylsulfanyl-3*H*-imidazol-4-yl]pyridin-2-ylamine

(2) as the key compound for the synthesis of a series of test compounds. Starting from 2, two different synthetic strategies yielded the 2-acylaminopyridin-4-ylimidazole derivatives 3–46 (Scheme 1). The target compounds were prepared using the carboxylic acid chlorides or the corresponding carboxylic acids after activation.



Scheme 1. Preparation of 2-acylaminopyridin-4-ylimidazole derivatives 3–46.

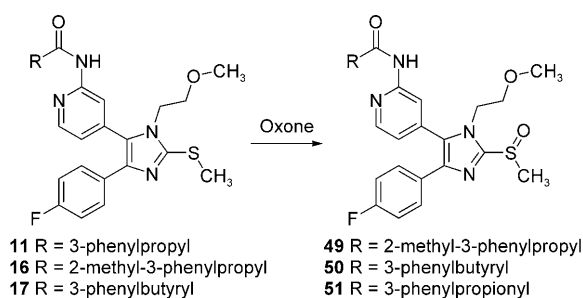
The first and notably fastest option to synthesize the target compounds was reaction of 2 with the respective carboxylic acid chlorides at room temperature using absolute pyridine as both a solvent and a base (general procedures A and B).<sup>[35]</sup> This procedure was limited by a disubstitution at the amino functionality which was described earlier.<sup>[33]</sup> This problem could be partly circumvented by using equimolar amounts of reactants, but disubstitution still occurred, and starting material remained unreacted. For each compound, optimum reaction conditions that balanced a molar excess of acid chloride with respect to starting material had to be defined. The development of a second method prevented this problem.<sup>[36]</sup> Activating the specific carboxylic acids with *N,N'*-carbonyldiimidazole (CDI) led to a reactive intermediate that could be easily converted into the 2-acylaminopyridin-4-ylimidazole derivatives by treatment with compound 2 in absolute tetrahydrofuran at room temperature or under reflux conditions (general procedure C).

As reported earlier, sulfoxides are expected as the main metabolites. Therefore, the sulfoxides of selected compounds were synthesized using Oxone® as an oxidant (general procedure D), as outlined in Scheme 2.

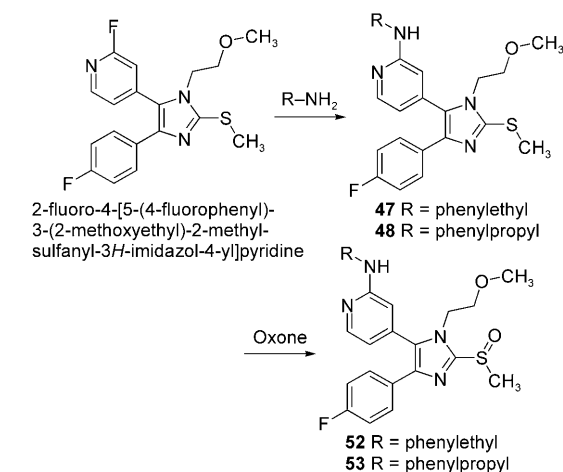
To facilitate comparison of the metabolic properties of the acylaminopyridines with the corresponding alkylaminopyridines, the respective compounds were synthesized by nucleophilic aromatic substitution from 2-fluoro-4-[5-(4-fluorophenyl)-3-(2-methoxyethyl)-2-methylsulfanyl-3*H*-imidazol-4-yl]pyridine as depicted in Scheme 3 (general procedure E).<sup>[29,37]</sup> The sulfoxides of the alkylaminopyridines were obtained according to general procedure D.

### Biological assays

The inhibitory potency of the compounds was evaluated using an immunosorbent non-radioactive p38 MAPK enzyme



Scheme 2. Preparation of sulfoxide derivatives 49–51.



Scheme 3. Preparation of 2-alkylaminopyridinylimidazoles 47 and 48 and the respective sulfoxides 52 and 53.

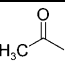
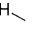
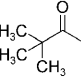
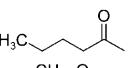
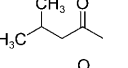
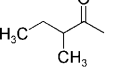
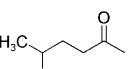
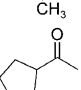
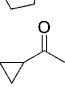
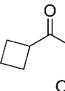
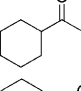
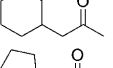
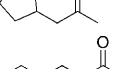
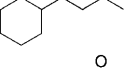
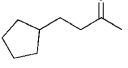
assay.<sup>[38]</sup> The ability of test compounds to compete with ATP for the kinase's ATP binding site correlates with the capacity of p38 MAPK to phosphorylate its natural substrate, activating transcription factor 2 (ATF2), when incubated with ATP and the test compound.

A second test system using human whole blood (HWB) takes physiological conditions into account. The anti-inflammatory activities of the compounds were determined by incubating lipopolysaccharide (LPS)-stimulated HWB with dilutions of the test compounds and determining the levels of released TNF $\alpha$  by ELISA technology.<sup>[39]</sup>

Previous experiments in the 2-alkylamino series identified small aliphatic residues as the most favorable substituents, as the respective test compounds showed high inhibitory potency.<sup>[29]</sup> In an initial approach to relate these results to the acyl series, we synthesized a number of 2-acylaminopyridine analogues with the respective small aliphatic residues (Table 2).

The IC<sub>50</sub> values obtained for compounds with small aliphatic acyl residues confirm the findings of the earlier study with the 2-alkylamino series. The residues were well tolerated and allowed the inhibitors to interact with the kinase's hydrophobic region II. Small aliphatic branched or linear residues as in 1 and 8, 9, 10, and 15 were also accepted (IC<sub>50</sub> values against p38 between 0.1 and 0.3  $\mu$ M), but a pivaloyl residue, as introduced in 7, was apparently too bulky (IC<sub>50</sub> = 1.76  $\mu$ M). For compounds with a terminal cyclic aliphatic group, the influence of

**Table 2.** Inhibition of p38 MAPK and inhibition of TNF $\alpha$  release: biological data for compounds with short aliphatic R groups and the amino compound 2.

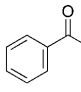
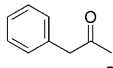
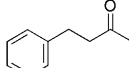
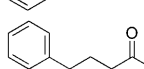
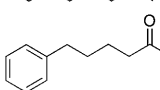
Compd	R <sup>[a]</sup>	IC <sub>50</sub> [ $\mu$ M]	
		p38 $\alpha$	TNF $\alpha$
1		0.108 $\pm$ 0.01	24.42 $\pm$ 5.82
2		1.424 $\pm$ 0.21	21.04 $\pm$ 3.14
7		1.759 $\pm$ 0.25	18.01 $\pm$ 7.02
8		0.083 $\pm$ 0.03	18.12 $\pm$ 0.20
9		0.103 $\pm$ 0.01	9.93 $\pm$ 1.89
10		0.311 $\pm$ 0.01	6.30 $\pm$ 2.33
15		0.179 $\pm$ 0.02	20.51 $\pm$ 5.83
21		0.458 $\pm$ 0.04	5.65 $\pm$ 1.54
22		0.128 $\pm$ 0.01	3.66 $\pm$ 0.448
23		0.116 $\pm$ 0.01	6.47 $\pm$ 0.878
25		0.156 $\pm$ 0.02	26.67 $\pm$ 2.17
26		0.219 $\pm$ 0.01	50.05 $\pm$ 9.78
27		0.108 $\pm$ 0.01	32.13 $\pm$ 10.50
28		0.196 $\pm$ 0.02	60.71 $\pm$ 1.97
29		0.224 $\pm$ 0.02	31.58 $\pm$ 1.05

[a] See Table 1 for the general structure.

the length of the connecting carbon chain was not so clear. The results for the compounds with terminal cyclopentyl rings (compounds **21**, **27**, and **29**) differ only slightly from the respective cyclohexyl analogues (compounds **25**, **26**, and **28**) in the p38 MAPK assay. In the TNF $\alpha$  assay, the cyclopropyl compound **22** was superior to the other inhibitors outlined in Table 3.

These encouraging results led to the design of a small series of compounds with terminal phenyl moieties on the acyl side chain (Table 3). The most potent inhibitor, compound **11**, featured a two-carbon spacer between the phenyl and amide groups, and had an IC<sub>50</sub> value in the kinase assay of 0.06  $\mu$ M. On the other hand, when considering the results of TNF $\alpha$  inhibition, either no (compound **3**, TNF $\alpha$  IC<sub>50</sub> = 8.1  $\mu$ M) or three

**Table 3.** Inhibition of p38 MAPK and inhibition of TNF $\alpha$  release: biological data for compounds with aromatic R groups.

Compd	R <sup>[a]</sup>	IC <sub>50</sub> [ $\mu$ M]	
		p38 $\alpha$	TNF $\alpha$
3		0.244 $\pm$ 0.01	8.079 $\pm$ 0.734
6		0.386 $\pm$ 0.02	23.44 $\pm$ 2.00
11		0.064 $\pm$ 0.01	36.97 $\pm$ 9.04
14		0.115 $\pm$ 0.02	5.798 $\pm$ 1.76
38		0.115 $\pm$ 0.02	10.25 % <sup>[b]</sup>

[a] See Table 1 for the general structure. [b] Percent inhibition at 10  $\mu$ M.

(compound **14**, TNF $\alpha$  IC<sub>50</sub> = 5.8  $\mu$ M) linker atoms in the side chain may be preferred.

We investigated the rigidity of the side chain, the introduction of methyl groups on the spacer carbons, or their replacement by oxygen (Table 4). A double bond in compound **13** or a cyclopropyl ring at the same position (compound **45**) rendered inhibitors with slightly higher IC<sub>50</sub> values in the enzyme assay than **11**, but slightly improved inhibition of TNF $\alpha$  release. Methyl groups on the spacer were well tolerated, again resulting in compounds with improved inhibition of TNF $\alpha$  release (compounds **16**, **17**, and **33**). When comparing compounds **33** and **34** and their racemic mixture **17**, it appears that the *R* configuration is preferred. One of the spacer carbons may be replaced by oxygen (compound **35**) with no deleterious effect, but a branched and bulky substituent at the neighboring position (compound **36**) is not tolerated. This finding is supported by a comparison of **36** with compound **9** (see above and Table 2).

The compounds depicted in Table 5 are analogues of **11** with substituents at the *para* position of the phenyl moiety. The *para* substituents were selected based on the observations of Craig.<sup>[40]</sup> However, *para* substituents with highly positive Hammett substituent constants (+ $\sigma$ ), as exemplified in **39**, should be avoided. Those with moderate  $\sigma$  and Hammett reaction ( $\rho$ ) constants result in low IC<sub>50</sub> values, as for compound **20**. Hence, **20**, with its low IC<sub>50</sub> value in the enzyme assay, indicated the *para*-methoxy group as the most favorable structure.

To investigate whether chain length or *para*-methoxy substitution have an impact on inhibitory potency, compounds **5**, **30**, and **31** (Table 6) were synthesized. These inhibitors contain a *para*-methoxyphenyl moiety and spacers of varying chain length. In this group, compound **20** again showed the lowest IC<sub>50</sub> value in the p38 enzyme assay. Hence, for further optimization, the two-carbon spacer of **20** was retained, and mono-, di-, and trisubstitution with the methoxy group was evaluated on the phenylpropionyl moiety (Table 7).

**Table 4.** Inhibition of p38 MAPK and inhibition of TNF $\alpha$  release: biological data for compounds with branched or rigid aromatic R groups.

Compd	R <sup>[a]</sup>	IC <sub>50</sub> [ $\mu$ M]	
		p38 $\alpha$	TNF $\alpha$
13		0.193 ± 0.07	30.64 ± 5.29
16		0.077 ± 0.01	21.93 ± 8.14
17		0.060 ± 0.01	21.38 ± 5.69
33		0.114 ± 0.03	10.20 ± 4.72
34		0.133 ± 0.03	37.08 ± 13.0
35		0.103 ± 0.01	30.70 ± 10.1
36		0.195 ± 0.09	9.850% ± 2.85% <sup>[b]</sup>
45		0.168 ± 0.04	24.58 ± 7.56

[a] See Table 1 for the general structure. [b] Percent inhibition at 10  $\mu$ M.

**Table 5.** Inhibition of p38 MAPK and inhibition of TNF $\alpha$  release: biological data for compounds with substituted *para*-phenylpropionic acid R groups.

Compd	R <sup>[a]</sup>	IC <sub>50</sub> [ $\mu$ M]	
		p38 $\alpha$	TNF $\alpha$
18		0.090 ± 0.01	58.47 ± 4.78
20		0.048 ± 0.01	37.60 ± 3.37
37		0.2542 ± 0.0854	NI <sup>[b]</sup>
39		0.220 ± 0.04	20.55 ± 3.15
46		2.447 ± 2.71	NI <sup>[b]</sup>

[a] See Table 1 for the general structure. [b] No inhibition.

**Table 6.** Inhibition of p38 MAPK and inhibition of TNF $\alpha$  release: biological data for compounds with substituted *para*-methoxyphenyl moieties in combination with various spacers.

Compd	R <sup>[a]</sup>	IC <sub>50</sub> [ $\mu$ M]	
		p38 $\alpha$	TNF $\alpha$
5		0.392 ± 0.09	14.45 ± 2.37
20		0.048 ± 0.01	37.60 ± 3.37
30		0.097 ± 0.02	15.58 ± 3.31
31		0.213 ± 0.01	24.94 ± 12.4

[a] See Table 1 for the general structure.

Di- and trisubstitution, as in **24**, **32**, **40**, **41**, and **44**, resulted in decreased inhibitory activity. Monosubstitution at the *para*, *ortho*, or *meta* positions, as in **20**, **42**, and **43**, led to highly potent p38 MAPK inhibition, with the *para*-substituted inhibitor **20** as the most promising candidate. Compound **20** was docked into the ATP binding site of p38 MAPK using PDB entry 1A9U as a template (Figure 2). The 4-fluorophenyl moiety penetrates deeply into the selectivity pocket (hydrophobic region I). A bidentate hydrogen bond anchors the molecule to the backbone Met 109. Pyridine N4 serves as an acceptor from the Met109 N–H group, and the Met109 carbonyl is an acceptor for the second hydrogen bond, whereas a third hydrogen bond is formed between the imidazole N1 and the terminal amino function of Lys53 (see also Figure 1).

The methoxyethyl moiety may interact with the ribose pocket of the ATP binding cleft. The acyl moiety interacts optimally with the hydrophobic region II in the area where the cleft opens to the cytosol. In this context, the *para*-methoxy moiety may be beneficial because it can interact with adjacent water molecules; in this way, it shields the hydrophobic region II from the surrounding polar solvent. A similar binding mode may be expected for the analogous compounds of this series.

In summary of the results of the biological assays, at the enzymatic level the greatest improvement in potency is observed by acetylation of the 2-aminopyridine derivate (compound **2** versus compound **1**: 13-fold improvement), whereas structural variations of the residue at the acyl group improved potency just over twofold (compound **1** versus compound **20**: 2.3-fold improvement). This may indicate that this part of the molecule has only a minor impact on interaction with the target. However, the effect can be explained by the surface topography of hydrophobic region II. Both domains of the kinase and hinge regions contribute to this region, where the ATP binding cleft opens up to the hydrophilic environment. Hence, structurally diverse residues are able to bind in more than one conformation. The fact that the two enantiomeric derivatives **33** and **34** show almost identical IC<sub>50</sub> values in the p38 MAPK assay is in



Compd	R <sup>[a]</sup>	IC <sub>50</sub> [μM]	
		p38α	TNFα
20		0.048 ± 0.01	37.60 ± 3.37
24		0.123 ± 0.01	54.26 ± 12.9
32		0.178 ± 0.02	54.93 ± 32.9
40		0.091 ± 0.02	25.08 ± 0.150
41		0.216 ± 0.04	44.67 ± 0.817
42		0.093 ± 0.01	26.92 ± 4.80
43		0.093 ± 0.01	26.92 ± 4.80
44		0.084 ± 0.02	19.75 ± 0.217

[a] See Table 1 for the general structure.

good agreement with this view. Unless structural variations on these residues might have only a minor impact on the optimization of potency toward blocking p38 MAPK activity, variations on this part of the molecule may allow additional optimization of the physicochemical properties of these inhibitors.

The introduction of an acyl moiety at the pyridine C2-amino position results, in almost all cases (41 of 43 compounds), in an improved inhibition of p38 MAPK in the enzyme assay. Only compounds **7** and **46**, both of which bear a bulky *tert*-butyl moiety, show a slightly potency toward p38 MAPK relative to the unsubstituted 2-aminopyridine **2**. The best compound of the series, compound **20**, shows a 30-fold improved inhibition of p38 MAPK relative to compound **2**. On the other hand, only a few (8 of 43) compounds show significantly better inhibition of LPS-stimulated TNFα release in the HWB test than that of **2**. This might be caused by plasma protein binding, weaker cell penetration, lower solubility, or a greater lipophilicity of com-

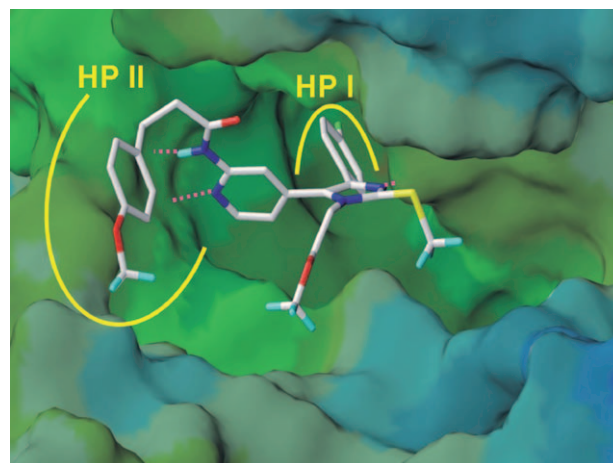


**Figure 2.** Compound **20** docked into the ATP binding site of p38 MAPK (template PDB code: 1A9U). The solvent-accessible Connolly surface is colored by lipophilicity (green: lipophilic; blue: hydrophilic). Hydrogen bonds are shown as purple dotted lines. Hydrophobic regions I (selectivity pocket) and II are indicated in yellow as HP I and HP II, respectively.

pounds with the acyl moiety. Stability can be ruled out as an explanation for this discrepancy, as the compounds tend to be stable under the assay conditions, as described below. There are a number of compounds that show the desired parallel improvement in enzyme inhibition and suppression of TNFα release: compounds **21**, **22**, and **23**, with their small aliphatic rings, and compound **10**, with a small aliphatic chain. Even a phenyl ring, as in compound **14**, is well tolerated on a three-carbon linker.

#### Determination of stability in HLM and HWB

In vitro metabolism assays can provide valuable information about the rate at which a compound is metabolized and the number and relative abundance of major metabolites produced. This information is valuable in predicting a drug candidate's likely duration of efficacy. Studies in liver microsomes can be used to provide this information.<sup>[41]</sup> Liver microsomes are subcellular fractions (mainly endoplasmic reticulum) containing many drug-metabolizing enzymes, such as cytochromes P450 (CYPs), flavin monooxygenases, carboxylesterases, and epoxide hydrolases. Liver microsomes therefore provide a convenient and inexpensive source of numerous enzyme functions that are mainly associated with phase I metabolism. The metabolic stabilities of selected test compounds **11** (representing the acyl series) and **47** (representing the alkyl series together with compound **48**) were investigated by using human liver microsomes (HLM). The compounds were incubated in the presence of a NADPH-regenerating system, and samples were analyzed at incubation times of 30 and 60 min in order to determine the time dependence and the extent of metabolism. RP-HPLC was used for analysis, and the main metabolites were identified by comparison of their retention times and UV spectra with those of synthesized reference compounds.

In the case of compound **11**, oxidation of sulfide to sulfoxide **49** is the predominant metabolic pathway (Table 8). After 30 min, the amount of residual non-metabolized compound **11** was only 20%, and decreased further to 11% after another

**Table 8.** 2-Acylaminopyridine **11** versus 2-alkylaminopyridine **47**: metabolic stability in human liver microsomes after 30 and 60 min incubation at 37 °C.

	<b>11</b>	<b>11</b>	<b>47</b>	<b>47</b>
Residual starting material	21%	11%	30%	21%
Sulfoxides <b>49</b> and <b>52</b>	20%	20%	10%	8%
Deacylated/dealkylated product <b>2</b>	2%	4%	12%	6%
Sulfoxide of deacylated/dealkylated product	–	–	2%	6%

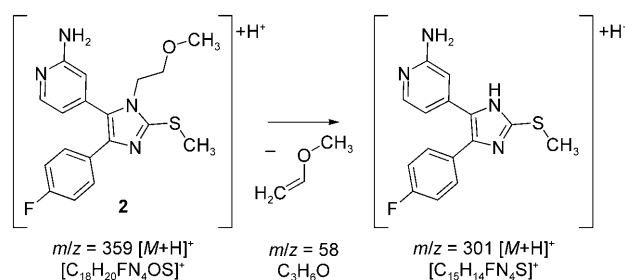
30 min. The concentration of sulfoxide remained at 20% after both 30 and 60 min. The deacylated metabolite was formed only to a very small extent (2%) after half an hour, but doubled after another 30 min. On one hand, the concentration of residual compound **47** remained at a higher level than in the case of **11**. But after 30 min, the dealkylation of **47** was sixfold more pronounced than deacylation of **11**. The respective metabolite was subject to further metabolism, resulting, for example, in the sulfoxide of the dealkylated compound (6% after 60 min). In summary, the 2-aminoalkyl derivatives are rapidly dealkylated, but the 2-aminoacyl residues appear to be more stable in HLM, as exemplified with the metabolic conversion of compounds **11** and **47** (Table 8) into compound **2**.

HWB stability data are usually correlated with a drug's distribution, metabolism, and excretion properties. Thus, whole-blood stability is routinely measured at multiple stages of the drug-discovery process. Interactions of a drug with enzymes such as nonspecific proteases and esterases, which are integral components of blood, can lead to chemical changes in the drug.<sup>[42,43]</sup> The stability of selected compounds **11** and **47** was assessed in lithium heparinized whole blood from three blood donors. After the addition of a test compound solution to whole blood and incubation for 10 or 30 min in an incubator (37 °C, 5% CO<sub>2</sub>, moisture-saturated atmosphere), the reaction mixture was centrifuged, and the proteins in the supernatant were precipitated by addition of acetonitrile. After a second centrifugation, the supernatant was analyzed by HPLC–MS–MS and selected reaction monitoring (SRM) for the presence of the respective deacylated or dealkylated products (Scheme 4). The results obtained from the HWB metabolism test differed from those obtained with isolated HLM. The MS–MS signals of tested compounds of both 2-acylaminopyridin-4-ylimidazoles and 2-alkylaminopyridin-4-ylimidazoles revealed extremely high metabolic stability under these test conditions. Therefore, in this case, there is no difference between the behaviors of **11** and **47** in HWB (Table 9).

## Conclusions

The structural class of tetrasubstituted 2-acylaminopyridin-4-ylimidazole-based p38 MAPK inhibitors was optimized by broad variation of the acyl moiety at position C2 of the pyridine ring.

We have shown that acylation of the 2-amino function of pyridine results in potent inhibition of p38 MAPK, similar to that of 2-alkylaminopyridin-4-ylimidazoles. Furthermore, a two-carbon spacer between the aminoacyl group and the terminal phenyl ring on the side chain provided the most potent inhibitor **11** (kinase assay) in this series. Moreover, compound **20** with its *para*-methoxyphenyl propionyl residue, exhibited high anti-inflammatory activity through potent inhibition of p38 MAPK. Widely varied acyl residues are very well tolerated, because



**Scheme 4.** Fragmentation of metabolite **2**.

**Table 9.** Stability of 2-acylaminopyridin-4-ylimidazole **11** and 2-alkylaminopyridin-4-ylimidazole **47** in HWB after incubation for 10 and 30 min.

Compd	Donor #	10 min Appearance of metabolite <b>2</b>	30 min Appearance of metabolite <b>2</b>
<b>11</b>	1	No deacylation	No deacylation
	2	No deacylation	No deacylation
	3	No deacylation	No deacylation
<b>47</b>	1	No dealkylation	No dealkylation
	2	No dealkylation	No dealkylation
	3	No dealkylation	No dealkylation

these residues interact optimally with the kinase's hydrophobic region II. Even sterically demanding compounds with branched side chains at the  $\alpha$  or  $\beta$  positions, or compounds with a heteroatom in the side chain are promising inhibitors. As a result, the inhibitory effect on p38 MAPK has greatly been improved relative to unsubstituted derivatives.

Our results show that the carbonyl function of 2-acylaminopyridin-4-ylimidazole is directly involved in the metabolic stability of this structural class of compounds, in contrast to the analogous 2-alkylaminopyridin-4-ylimidazoles. Both structural classes are stable in HWB. The introduction of acyl side chains at C2 of the pyridine moiety leads to promising new candidates that inhibit p38 MAPK in the low-nanomolar range. These substitution patterns provide for the creation of potent new p38 MAPK inhibitors with high affinity for the enzyme and improved metabolic stability.

## Experimental Section

### General

All reagents and solvents were of commercial quality and used without further purification. HWB from three donors was kindly provided by Blutbank/UKT (University Hospital Tübingen, Germany). Water was used from an in-house bi-distillation device. HLM provided by c-a-i-r biosciences GmbH (Tübingen, Germany) were used. These microsomes were characterized for protein and cytochrome P450 content (protein: 19.13 mg mL<sup>-1</sup>; CYP450: 190.5 pmol mg<sup>-1</sup>).

### Molecular modeling

Structure **20** was built with Sybyl v. 7.1, minimized under MMFF94 force-field conditions, and subsequently docked manually into the ATP binding site of p38 MAPK. The crystal structure of p38 MAPK with SB 203580 was used as a template (PDB code: 1A9U). To take the conformational flexibility of the protein into account, the assembly of kinase and inhibitor was then minimized again, excluding from the calculation all protein atoms outside a sphere of 12 Å radius around the inhibitor (Sybyl v. 7.1, Tripos Inc., St. Louis, MO, USA).

### Incubations

**The HLM incubations** (final total volume: 500 µL) of 2.5 µL were made in the presence of an NADPH-regenerating system and 80 mM MgCl<sub>2</sub>·H<sub>2</sub>O in 0.1 M Tris buffer (pH 7.4). After pre-incubation for 5 min in a shaking water bath (37 °C, 50 rpm), the reaction was started by the addition of microsomes at various time points (0, 30, and 60 min). The reaction tubes for 0 min were directly put on ice. To stop the reaction after 30 or 60 min, the tubes were put on ice, and cold CH<sub>3</sub>CN (125 µL each) was added. After centrifugation (5 min, 13000 rpm, 4 °C), supernatant (100 µL) was withdrawn from each tube and transferred into a 300 µL HPLC vial and frozen at -20 °C until analysis.

**The HWB incubations.** HWB (500 µL) from three different donors was pre-incubated at 37 °C in disposable reaction tubes in a shaking water bath. Stock solutions A of the test compounds (10 mM) were prepared in CH<sub>3</sub>OH. The first dilution B was prepared in 10% CrEL®/EtOH/DPBS buffer (450 µL) and stock solution A (50 µL), to give 1000 µM stock solution B. 150 µL of these solutions B were diluted in 350 µL 10% CrEL®/EtOH/DPBS buffer to give a 300 mM working solution. Working solutions (5 µL each) were added to the blood and mixed carefully (end concentration: 3 mM). The samples were incubated for 10 and 30 min at 37 °C in an incubator (37 °C, 5% CO<sub>2</sub>, moisture-saturated atmosphere). The reaction tubes for 0 min were directly put on ice. To stop the reaction after 10 or 30 min, the tubes were put on ice and centrifuged (12 min, 13000 rpm, 4 °C). Supernatants (200 µL each) were withdrawn and transferred into a reaction tube containing 600 µL cold CH<sub>3</sub>CN. The samples were centrifuged once more (12 min, 40000 rpm, 4 °C). The resulting supernatants (100 µL each) was transferred into a 300 µL HPLC vial and frozen at -20 °C until analysis.

### Chemical analysis

Melting points were determined on a Büchi Melting Point B-545 apparatus and are thermodynamically corrected. <sup>1</sup>H and <sup>13</sup>C NMR spectra were collected on a Bruker Advance Spectrospin AC 200 at

200 and 50 MHz, respectively. Chemical shifts (δ) are reported in ppm. Mass spectra were recorded on a Finnigan Triple-Stage Quadrupole (TSQ-70). HPLC data were determined on an HP 1090 instrument (Thermo Betasil C<sub>8</sub> column [150×4.6 mm, dp=5 µm]). HPLC results are given as retention times (min) and relative purity (%). TLC analyses were performed on fluorescent silica gel 60 plates (Macherey–Nagel, No. 818133) and on fluorescent RP-18 plates (Merck, No. 1.05559.0001); spots were visualized under UV illumination at 254 and 366 nm.

**N-[4-[5-(4-Fluorophenyl)-3-(2-methoxyethyl)-2-methylsulfanyl-3H-imidazol-4-yl]pyridin-2-yl]acetamide (1):** K<sub>2</sub>CO<sub>3</sub> (6.4 g, 46.6 mmol, 1.0 equiv) was added to a solution of N-[4-[5-(4-fluorophenyl)-3-(2-methoxyethyl)-2-thio-2,3-dihydro-1H-imidazol-4-yl]pyridin-2-yl]acetamide (18.0 g, 46.6 mmol, 1.0 equiv) in 50 mL CH<sub>3</sub>OH, then CH<sub>3</sub>I (8.54 g, 60.6 mmol, 1.3 equiv) was added via dropping funnel. The reaction mixture was stirred for 18 h at room temperature. After reaction completion, the solids were separated by vacuum filtration, and the filtrate was concentrated in vacuo to give a white solid (14.0 g, 35.0 mmol, 75%); mp: 150 °C; <sup>1</sup>H NMR (CDCl<sub>3</sub>): δ = 2.22 (s, 3H, COCH<sub>3</sub>), 2.72 (s, 3H, SCH<sub>3</sub>), 3.24 (s, 3H, OCH<sub>3</sub>), 3.51 (t, 2H, J = 6.0 Hz, OCH<sub>2</sub>), 4.09 (t, 2H, J = 5.9 Hz, NCH<sub>2</sub>), 6.86–6.98 (m, 3H, 4-F-Ph, Pyr), 7.37–7.44 (m, 2H, 4-F-Ph), 8.25–8.28 (m, 2H, Pyr), 8.70 (s, 1H, NH); <sup>13</sup>C NMR (CDCl<sub>3</sub>): δ = 16.3 (SCH<sub>3</sub>), 24.6 (COCH<sub>3</sub>), 44.2 (NCH<sub>2</sub>), 58.8 (OCH<sub>3</sub>), 70.6 (OCH<sub>2</sub>), 115.0 (d, <sup>2</sup>J<sub>(C,F)</sub> = 21.3 Hz, C3 and C5 4-F-Ph), 115.1 (Aryl), 121.6 (Aryl), 127.3 (Aryl), 128.8 (d, <sup>3</sup>J<sub>(C,F)</sub> = 7.9 Hz, C2 and C6 4-F-Ph), 129.9 (d, <sup>4</sup>J<sub>(C,F)</sub> = 3.3 Hz, C1 4-F-Ph), 138.9 (Aryl), 141.4 (Aryl), 144.8 (Aryl), 148.1 (Aryl), 152.1 (Aryl), 161.8 (d, <sup>1</sup>J<sub>(C,F)</sub> = 244.5 Hz, C4 4-F-Ph), 168.7 (CO); FTIR (ATR):  $\tilde{\nu}$  = 1668, 1542, 1504, 1432, 1415, 1273, 1120, 1110, 845, 819 cm<sup>-1</sup>; HPLC: t<sub>R</sub> = 5.8 min (96% purity); MS (ESI): m/z = 401.1 [M+H]<sup>+</sup>.

**4-[5-(4-Fluorophenyl)-3-(2-methoxyethyl)-2-methylsulfanyl-3H-imidazol-4-yl]pyridin-2-ylamine (2):** Compound **1** (13.4 g, 33.5 mmol, 1.0 equiv) was added to HCl<sub>(aq)</sub> (10%, 300 mL), stirred for 20 min at room temperature, and then heated for 5 h at reflux. Upon reaction completion, the mixture was cooled in an ice bath and brought to pH 8 with an aqueous solution of NaOH (20% m/m) to form a precipitate, which was collected by vacuum filtration. Subsequent recrystallization (diisopropyl ether) gave a yellow solid (10.0 g, 27.9 mmol, 83%); mp: 130 °C; <sup>1</sup>H NMR (CDCl<sub>3</sub>): δ = 2.71 (s, 3H, SCH<sub>3</sub>), 3.25 (s, 3H, OCH<sub>3</sub>), 3.48 (t, 2H, J = 6.0 Hz, OCH<sub>2</sub>), 4.03 (t, 2H, J = 5.9 Hz, NCH<sub>2</sub>), 4.48 (s, 2H, NH<sub>2</sub>), 6.46 (s, 1H, Pyr), 6.61 (d, 1H, J = 5.2 Hz, Pyr), 6.88–6.97 (m, 2H, 4-F-Ph), 7.42–7.49 (m, 2H, 4-F-Ph), 8.12 (d, 1H, J = 5.2 Hz, Pyr); <sup>13</sup>C NMR (CDCl<sub>3</sub>): δ = 16.3 (SCH<sub>3</sub>), 44.0 (NCH<sub>2</sub>), 58.8 (OCH<sub>3</sub>), 70.6 (OCH<sub>2</sub>), 109.9 (Aryl), 114.8 (Aryl), 115.4 (d, <sup>2</sup>J<sub>(C,F)</sub> = 21.4 Hz, C3 and C5 4-F-Ph), 127.8 (Aryl), 128.5 (d, <sup>3</sup>J<sub>(C,F)</sub> = 7.9 Hz, C2 and C6 4-F-Ph), 130.0 (d, <sup>4</sup>J<sub>(C,F)</sub> = 3.2 Hz, C1 4-F-Ph), 138.1 (Aryl), 140.6 (Aryl), 144.1 (Aryl), 148.9 (Aryl), 158.9 (Aryl), 161.7 (d, <sup>1</sup>J<sub>(C,F)</sub> = 244.1 Hz, C4 4-F-Ph); FTIR (ATR)  $\tilde{\nu}$  = 1614, 1543, 1510, 1485, 1443, 1225, 1118, 845, 815, 691 cm<sup>-1</sup>; HPLC: t<sub>R</sub> = 3.6 min (100% purity); MS (ESI): m/z = 359.1 [M+H]<sup>+</sup>.

**General procedure A:** The respective carboxylic acid chloride was added to a solution of **9** in dry pyridine under an argon atmosphere. The reaction was allowed to proceed until TLC analysis indicated complete conversion. After removing the solvent in vacuo, EtOAc was added to the residue. The organic layer was washed with H<sub>2</sub>O, dried over Na<sub>2</sub>SO<sub>4</sub>, and concentrated in vacuo.

**General procedure B:** Under an argon atmosphere, **9** was dissolved in dry THF, and freshly distilled Et<sub>3</sub>N was added. The mixture was cooled in an ice bath, and the respective carboxylic acid chloride was added. The reaction mixture was stirred at room temperature until TLC analysis indicated complete conversion. After remov-



ing the solvent in vacuo, EtOAc was added to the residue. The organic layer was washed with H<sub>2</sub>O, dried over Na<sub>2</sub>SO<sub>4</sub>, and concentrated in vacuo.

**General procedure C:** Under an argon atmosphere, *N,N'*-carbonyldiimidazole was added to a stirred solution of the respective carboxylic acid in dry THF at room temperature. When gas evolution ceased, **9** was added, and the reaction was allowed to proceed at room temperature until complete conversion. After removing the solvent in vacuo, EtOAc was added to the residue. The organic layer was washed with H<sub>2</sub>O, dried over Na<sub>2</sub>SO<sub>4</sub>, and concentrated in vacuo.

**General procedure D:** The specific 2-acyl- or 2-alkylaminopyridinyl compound was dissolved in THF, and H<sub>2</sub>O was added. The mixture was cooled in an ice bath, and an aqueous solution of Oxone® was added dropwise; the resulting mixture was stirred at 0 °C. After reaction completion, the solution was allowed to warm to room temperature. An aqueous saturated solution of NaHCO<sub>3</sub> was added, and the mixture was extracted with EtOAc. The organic layer was washed with H<sub>2</sub>O and brine, dried over Na<sub>2</sub>SO<sub>4</sub>, and concentrated in vacuo.

**General procedure E:** 2-Fluoro-4-[5-(4-fluorophenyl)-3-(2-methoxyethyl)-2-methylsulfanyl-3*H*-imidazol-4-yl]pyridine and the specific amine were stirred at 160 °C. Excess amine was removed by vacuum distillation, and the residue was dissolved in EtOAc and washed with an aqueous saturated solution of NaHCO<sub>3</sub>, then with H<sub>2</sub>O and brine. The organic layer was dried over Na<sub>2</sub>SO<sub>4</sub> and concentrated in vacuo.

## Acknowledgements

This work was financially supported by the ratiopharm Group and Fonds der Chemischen Industrie. The authors thank Dr. D. Domeyer for molecular modeling and Dr. S. Luik, K. Bauer, and M. Goertter for their assistance in biological testing. Dr. D. Bullinger, Dr. B. Kammerer, C. Mayer, and Dr. H. Scheible are kindly acknowledged for collecting LC-MS data. Thanks also to Pierre Koch for helpful discussions of the biological data.

**Keywords:** cytokines · imidazoles · inhibitors · p38 MAP kinase · pyridines

- [1] S. Kumar, J. Boehm, J. C. Lee, *Nat. Rev. Drug Discovery* **2003**, *2*, 717–726.
- [2] J. S. Smolen, G. Steiner, *Nat. Rev. Drug Discovery* **2003**, *2*, 473–488.
- [3] M. L. Foster, F. Halley, J. E. Souness, *Drug News Perspect.* **2000**, *13*, 488–497.
- [4] B. Bresnihan, J. M. Alvaro-Gracia, M. Cobby, M. Doherty, Z. Domljan, P. Emery, G. Nuki, K. Pavelka, R. Rau, B. Rozman, I. Watt, B. Williams, R. Aitchison, D. McCabe, P. Musick, *Arthritis Rheum.* **1998**, *41*, 2196–2204.
- [5] G. R. Burmester, X. Mariette, C. Montecucco, I. Monteagudo-Saez, M. Malaise, A. G. Tzioufas, J. W. J. Bijlsma, K. Unnebrink, S. Kary, H. Kupper, *Ann. Rheum. Dis.* **2007**, *66*, 732–739.
- [6] S. Cohen, E. Hurd, J. Cush, M. Schiff, M. E. Weinblatt, L. W. Moreland, J. Kremer, M. B. Bear, W. J. Rich, D. McCabe, *Arthritis Rheum.* **2002**, *45*, 614–624.
- [7] S. B. Cohen, P. Emery, M. W. Greenwald, M. Dougados, R. A. Furie, M. C. Genovese, E. C. Keystone, J. E. Loveless, G. R. Burmester, M. W. Cravets, E. W. Hesse, T. Shaw, M. C. Todoritis, *Arthritis Rheum.* **2006**, *49*, 2793–2806.
- [8] J. C. W. Edwards, L. Szczepanski, J. Szechinski, A. Filipowicz-Sosnowska, P. Emery, D. R. Close, R. M. Stevens, T. Shaw, *New Engl. J. Med.* **2004**, *350*, 2572–2581.
- [9] D. T. Felson, J. J. Anderson, M. Boers, C. Bombardier, D. Furst, C. Goldsmith, L. M. Katz, R. Lightfoot, Jr., H. Paulus, V. Strand, *Arthritis Rheum.* **1995**, *38*, 727–735.
- [10] J. L. Kaine, *Curr. Ther. Res.* **2007**, *68*, 379–399.
- [11] L. Klareskog, D. van der Heijde, J. P. de Jager, A. Gough, J. Kalden, M. Malaise, E. Martin Mola, K. Pavelka, J. Sany, L. Settas, J. Wajdula, R. Pedersen, S. Fatenejad, M. Sanda, *Lancet* **2004**, *363*, 675–681.
- [12] J. M. Kremer, R. Westhovens, M. Leon, E. Di Giorgio, R. Alten, S. Steinfeld, A. Russell, M. Dougados, P. Emery, I. F. Nuamah, G. R. Williams, J. C. Becker, D. T. Hagerty, L. W. Moreland, *New Engl. J. Med.* **2003**, *349*, 1907–1915.
- [13] R. N. Maini, P. C. Taylor, J. Szechinski, K. Pavelka, J. Bröll, G. Balint, P. Emery, F. Raemen, J. Petersen, J. Smolen, D. Thomson, T. Kishimoto, *Arthritis Rheum.* **2006**, *49*, 2817–2829.
- [14] R. Maini, E. W. St. Clair, F. Breedveld, D. Furst, J. Kalden, M. Weisman, J. Smolen, P. Emery, G. Harriman, M. Feldmann, P. Lipsky, *Lancet* **1999**, *354*, 1932–1939.
- [15] N. Nishimoto, K. Yoshizaki, N. Miyasaka, K. Yamamoto, S. Kawai, T. Takeuchi, J. Hashimoto, J. Azuma, T. Kishimoto, *Arthritis Rheum.* **2004**, *47*, 1761–1769.
- [16] N. Nishimoto, J. Hashimoto, N. Miyasaka, K. Yamamoto, S. Kawai, T. Takeuchi, N. Murata, D. van der Heijde, T. Kishimoto, *Ann. Rheum. Dis.* **2007**, *66*, 1162–1167.
- [17] E. W. St. Clair, D. M. van der Heijde, J. S. Smolen, R. N. Maini, J. M. Bathon, P. Emery, E. Keystone, M. Schiff, J. R. Kalden, B. Wang, K. Dewoody, R. Weiss, D. Baker, *Arthritis Rheum.* **2004**, *47*, 3432–3443.
- [18] E. H. Choy, G. S. Panayi, *New Engl. J. Med.* **2001**, *344*, 907–916.
- [19] C. Sheridan, *Nat. Biotechnol.* **2008**, *26*, 143–144.
- [20] G. L. Schieven, *Curr. Top. Med. Chem.* **2005**, *5*, 921–928.
- [21] M. D. Köller, *Wien. Med. Wochenschr.* **2006**, *156*, 53–60.
- [22] S. A. Laufer, W. Zimmermann, K. J. Ruff, *J. Med. Chem.* **2004**, *47*, 6311–6325.
- [23] K. P. Wilson, P. G. McCaffrey, K. Hsiao, S. Pazhinisamy, V. Galullo, G. W. Bemis, M. J. Fitzgibbon, P. R. Caron, M. A. Murcko, M. S. S. Su, *Chem. Biol.* **1997**, *4*, 423–431.
- [24] J. L. Adams, T. F. Gallagher, J. C. Boehm, S. Kassis, P. D. Gorycki, R. J. Gum, E. F. Webb, M. E. Sorenson, J. M. Smietana, R. S. Garigipati, R. F. Hall, A. Ayrton, A. Badger, D. E. Griswold, P. R. Young, J. C. Lee, *Special Publication—Royal Society of Chemistry* **2001**, *264*, 163–173.
- [25] R. J. Gum, M. M. McLaughlin, S. Kumar, Z. Wang, M. J. Bower, J. C. Lee, J. L. Adams, G. P. Livi, E. J. Goldsmith, P. R. Young, *J. Biol. Chem.* **1998**, *273*, 15605–15610.
- [26] Z. Wang, B. J. Canagarajah, J. C. Boehm, S. Kassis, M. H. Cobb, P. R. Young, S. Abdel-Meguid, J. L. Adams, E. J. Goldsmith, *Structure* **1998**, *6*, 1117–1128.
- [27] P. Traxler, *Expert Opin. Ther. Pat.* **1998**, *8*, 1599–1625.
- [28] S. A. Laufer, G. K. Wagner, D. A. Kotschenreuther, W. Albrecht, *J. Med. Chem.* **2003**, *46*, 3230–3244.
- [29] S. A. Laufer, D. R. J. Hauser, D. M. Domeyer, K. Kinkel, A. J. Liedtke, *J. Med. Chem.* **2008**, *51*, 4122–4149.
- [30] C. E. Fitzgerald, S. B. Patel, J. W. Becker, P. M. Cameron, D. Zaller, V. B. Piskounis, S. J. O'Keefe, G. Scapin, *Nat. Struct. Biol.* **2003**, *10*, 764–769.
- [31] B. Kammerer, H. Scheible, G. Zurek, M. Godejohann, K. P. Zeller, C. H. Gleiter, W. Albrecht, S. Laufer, *Xenobiotica* **2007**, *37*, 280–297.
- [32] B. Kammerer, H. Scheible, W. Albrecht, C. H. Gleiter, S. Laufer, *Drug Metab. Dispos.* **2007**, *35*, 875–883.
- [33] S. Miwatashi, Y. Arikawa, E. Kotani, M. Miyamoto, K. Naruo, H. Kimura, T. Tanaka, S. Asahi, S. Ohkawa, *J. Med. Chem.* **2005**, *48*, 5966–5979.
- [34] G. K. Wagner, D. Kotschenreuther, W. Zimmermann, S. A. Laufer, *J. Org. Chem.* **2003**, *68*, 4527–4530.
- [35] S. A. Filla, B. M. Mathes, K. W. Johnson, L. A. Phebus, M. L. Cohen, D. L. Nelson, J. M. Zgombick, J. A. Erickson, K. W. Schenck, D. B. Wainscott, T. A. Brancheck, J. M. Schaus, *J. Med. Chem.* **2003**, *46*, 3060–3071.
- [36] H. A. Staab, *Angew. Chem.* **1962**, *74*, 407–423.
- [37] S. A. Laufer, D. R. J. Hauser, A. J. Liedtke, *Synthesis* **2008**, 253–266.
- [38] S. A. Laufer, S. Thuma, C. Peifer, C. Greim, Y. Herweh, A. Albrecht, F. Dehner, *Anal. Biochem.* **2005**, *344*, 135–137.
- [39] C. T. Damsgaard, L. Lauritzen, P. C. Calder, T. M. R. Kjaer, H. Frokiaer, *J. Immunol. Methods* **2009**, *340*, 95–101.
- [40] P. N. Craig, *J. Med. Chem.* **1971**, *14*, 680–684.

- [41] R. E. Pearce, C. J. McIntyre, A. Madan, U. Sanzgiri, A. J. Draper, P. L. Bullock, D. C. Cook, L. A. Burton, J. Latham, *Arch. Biochem. Biophys.* **1996**, *331*, 145–149.
- [42] R. M. Lindsay, W. R. Fox, J. D. Baty, R. G. Willis, *Biochem. Pharmacol.* **1991**, *41*, 1671–1678.
- [43] B. Li, M. Sedlacek, I. Manoharan, R. Boopathy, E. G. Duysen, P. Masson, O. Lockridge, *Biochem. Pharmacol.* **2005**, *70*, 1673–1684.

---

Received: June 19, 2009

Revised: August 17, 2009

Published online on September 3, 2009